

Supplementary Material (ESI) for Journal of Materials Chemistry  
This journal is (c) The Royal Society of Chemistry 2011

**Supporting Information for**

**Controlled Synthesis and Upconversion Luminescence of Lanthanide Doped BaYF<sub>5</sub> Nanocrystals**

**Hailong Qiu,<sup>a</sup> Guanying Chen,<sup>a,b</sup> Liang Sun,<sup>a</sup> Shuwei Hao<sup>a</sup> Gang Han,<sup>c\*</sup> and Chunhui Yang<sup>a\*</sup>**

<sup>a</sup>School of Chemical Engineering and Technology, Harbin Institute of Technology, Harbin 150001, People's Republic of China. \*E-mail:yangchh@hit.edu.cn

<sup>b</sup>Institute for Lasers, Photonics and Biophotonics, Department of Chemistry, University at Buffalo, The State University of New York, Buffalo, New York 14260.

<sup>c</sup>Department of Biochemistry and Molecular Pharmacology, University of Massachusetts Medical School, Worcester, Massachusetts 01605. \*E-mail: gang.han@umassmed.edu.

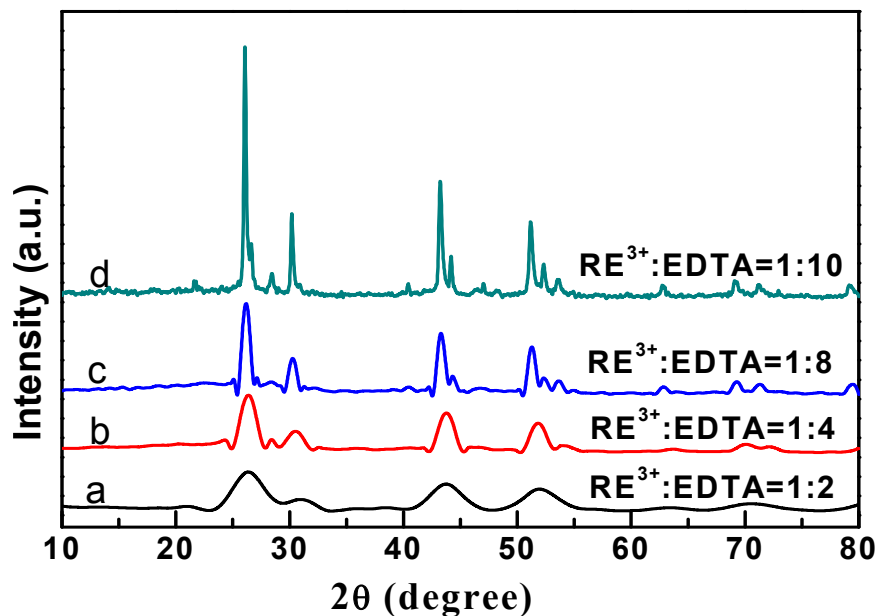


**Figure S1.** The typical XRD patterns of BaYF<sub>5</sub> with the RE<sup>3+</sup>/EDTA of (a)1:2, (b)1:4, (c)1:8, and (d)1:10, respectively.

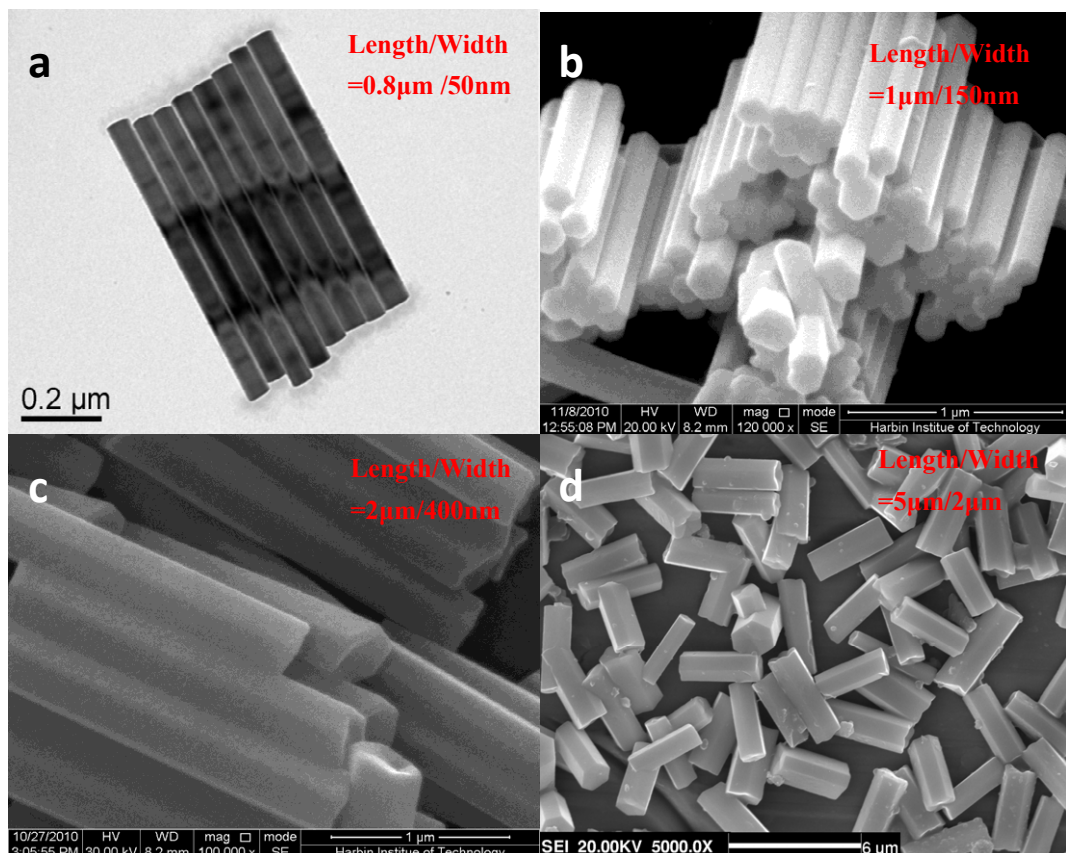


**Figure S2.** (a) TEM, (b, c and d) FESEM images of  $\text{NaYF}_4$  with the  $\text{RE}^{3+}/\text{EDTA}$  of (a)1:10, (b)1:8, (c)1:4, and (d)1:2, respectively. (f) XRD patterns of  $\text{NaYF}_4$  powders in Figure S2 (a-d). All the diffraction peaks of  $\text{NaYF}_4$  powders with  $\text{RE}^{3+}/\text{EDTA}$  of (a)1:10, (b)1:8, (c)1:4, and (d)1:2 agree well with standard hexagonal structure of JCPDS 16-0334.

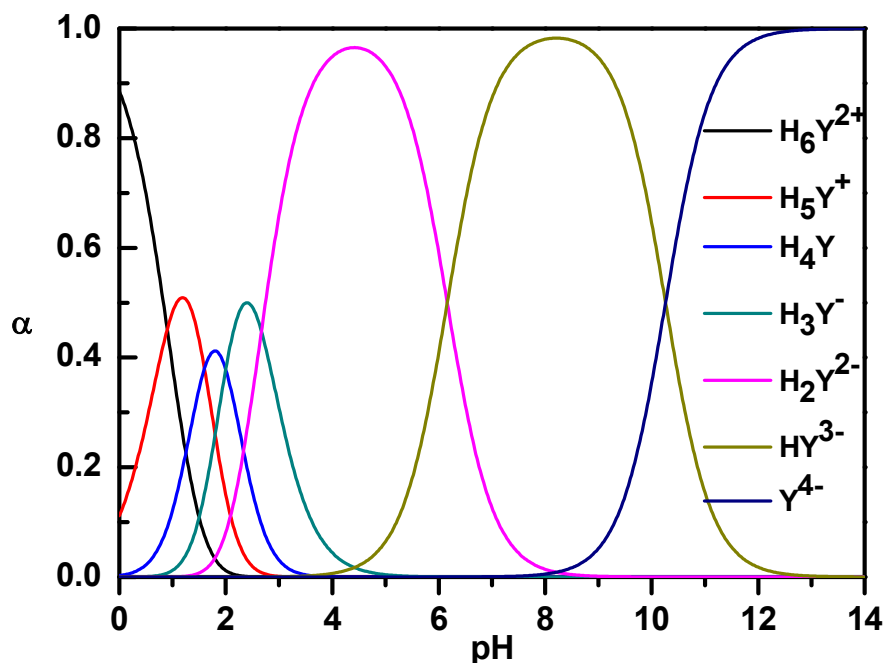


**Figure S3.** Relative distribution of species of EDTA versus the pH value.

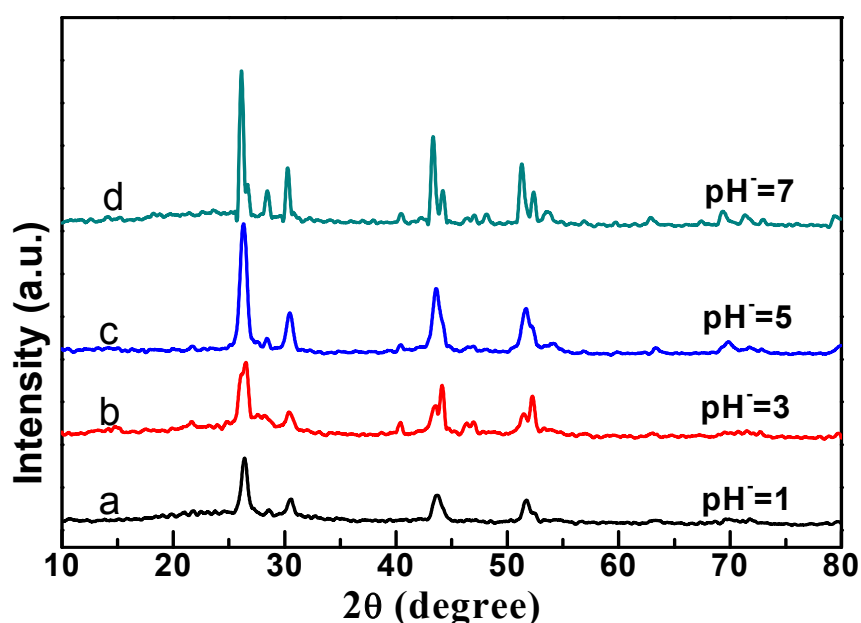


**Figure S4.** The typical XRD patterns of  $\text{BaYF}_5$  at (a)  $\text{pH}=1$ , (b) $\text{pH}=3$ , (c)  $\text{pH}=5$ , and (d)  $\text{pH}=7$ , respectively

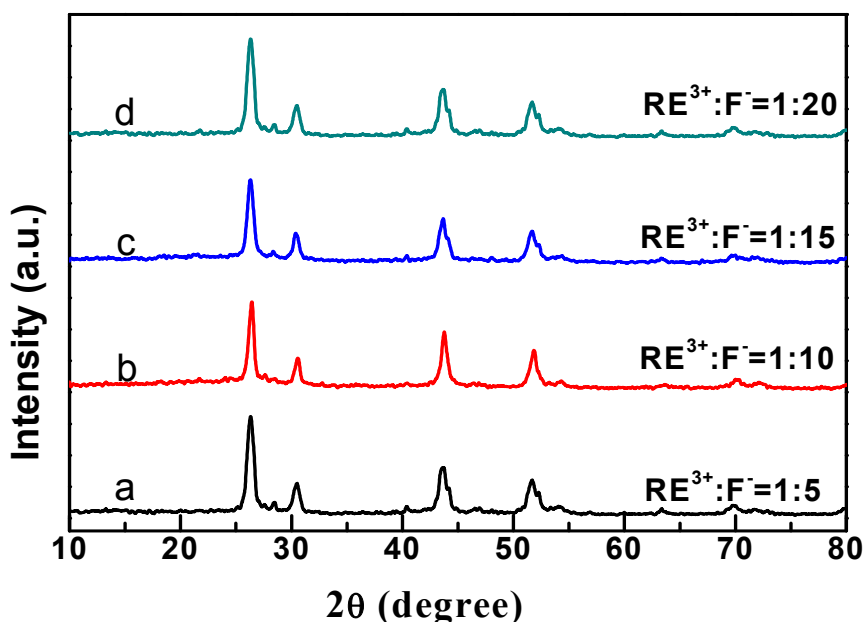


**Figure S5.** The typical XRD patterns of  $\text{BaYF}_5$  with  $\text{RE}^{3+}/\text{F}^-$  ratio of (a) 1:5 (b) 1:10, (c) 1:15 and (d) 1:20, respectively.

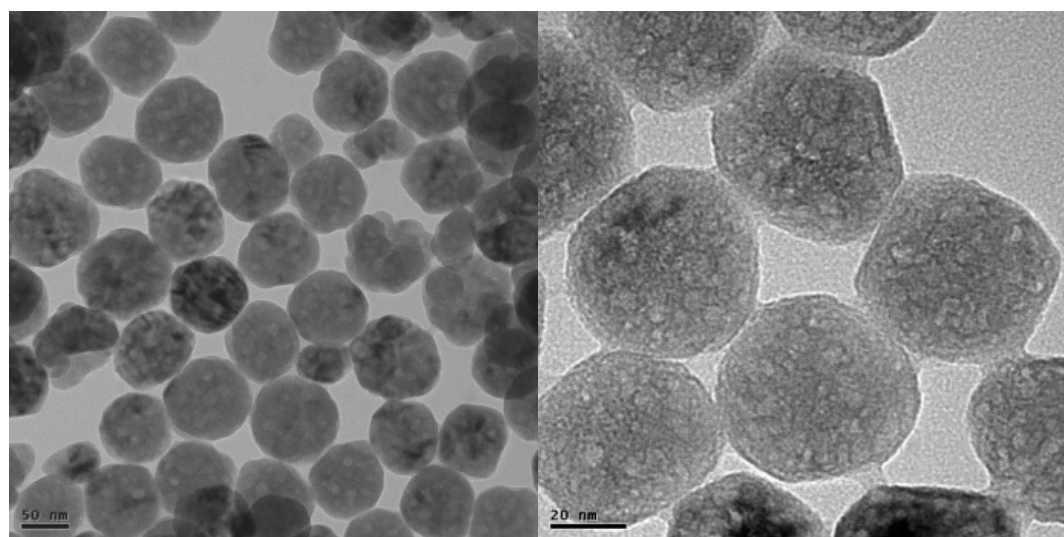


**Figure S6.** TEM images of  $\text{BaYF}_5$  nanocrystals after ligand exchange.

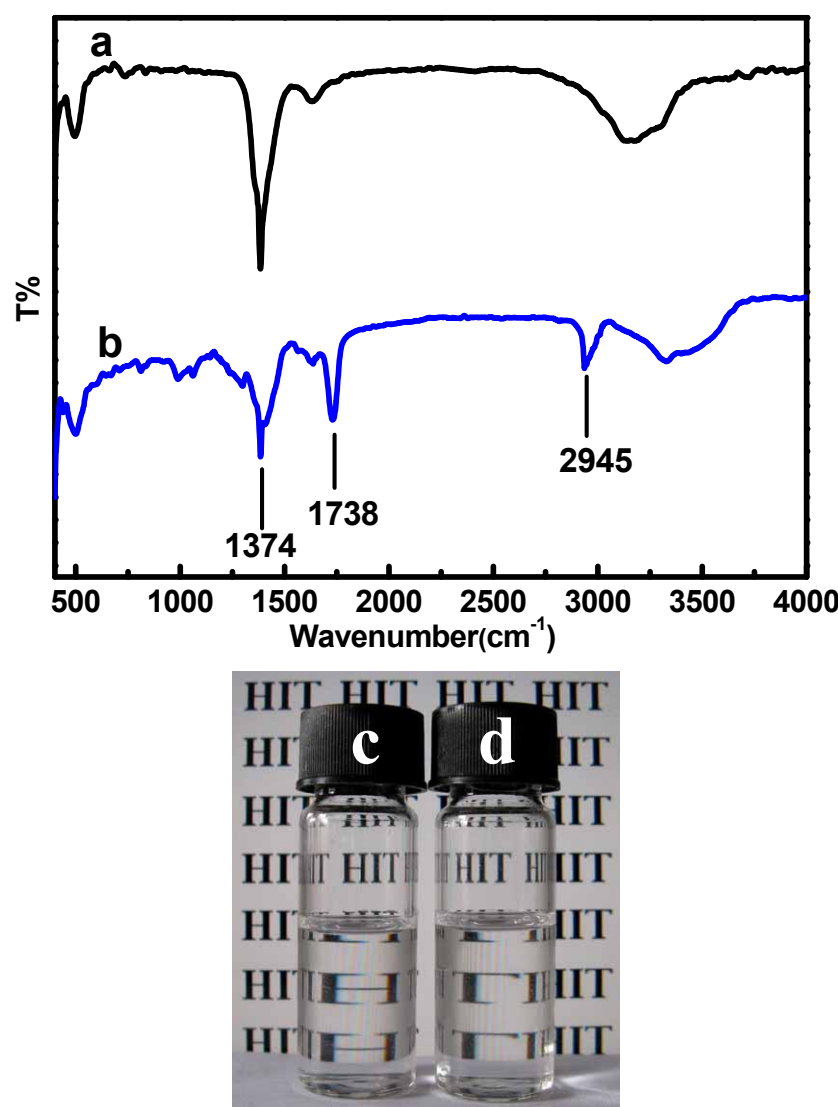


**Figure S7.** Fourier transform infrared (FT-IR) spectra of  $\text{BaYF}_5$  nanocrystals before (a) and after (b) ligand exchange using PAA. Photographs of colloidal solutions of the  $\text{BaYF}_5$  nanocrystals (50-60nm) dispersed in cyclohexane and water before (c) and after (d) PAA modification. The FT-IR spectra were used to characterize the functional groups present on the surface of nanocrystals. The band at  $1374\text{ cm}^{-1}$  characterizing the mode of the  $\text{C=O}$  ( $\text{N-CO-OH}$ ) stretching vibration in the EDTA molecule became weaker after ligand exchange (Figure S7b), suggesting the decreased EDTA molecule on the surface of  $\text{BaYF}_5$  nanoparticles. Moreover, the bands at  $1738\text{ cm}^{-1}$  and  $2945\text{ cm}^{-1}$  newly appeared in Figure S7b characterize the  $-\text{COOH}$  group and the stretching vibration of methylene ( $\text{CH}_2$ ) in the long alkyl chain, respectively, illustrating the presence of the PAA molecule on the surface of  $\text{BaYF}_5$  nanoparticles. These observations give a strong evidence of the successful exchange of EDTA by the ligand of PAA. The broad band between  $2800\text{ cm}^{-1}$  and  $3600\text{ cm}^{-1}$  arises from the O-H stretching vibration ( $\text{COO-H}$ ).

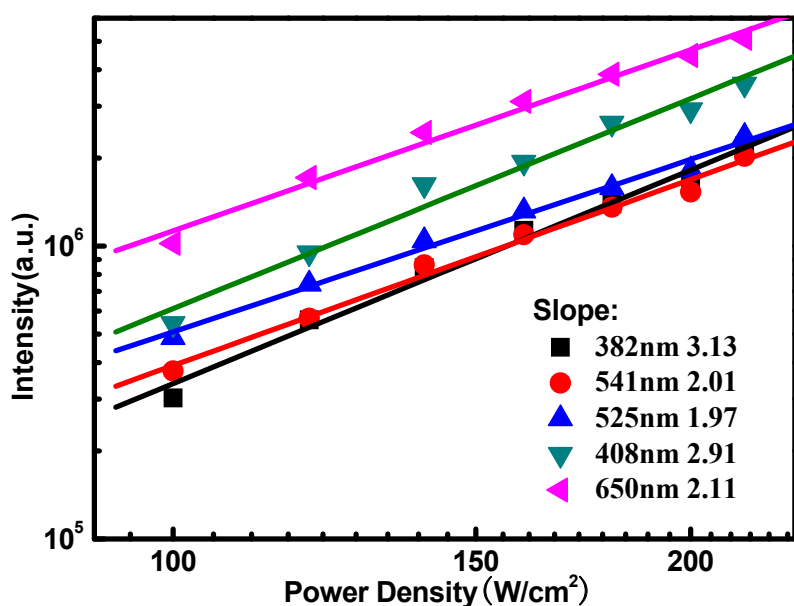


**Figure S8.** The dependence of the intensities of upconversion emissions bands on the power of excitation at 980 nm in the  $\text{BaYF}_5$ : 18% $\text{Yb}^{3+}$ /2% $\text{Er}^{3+}$  system.

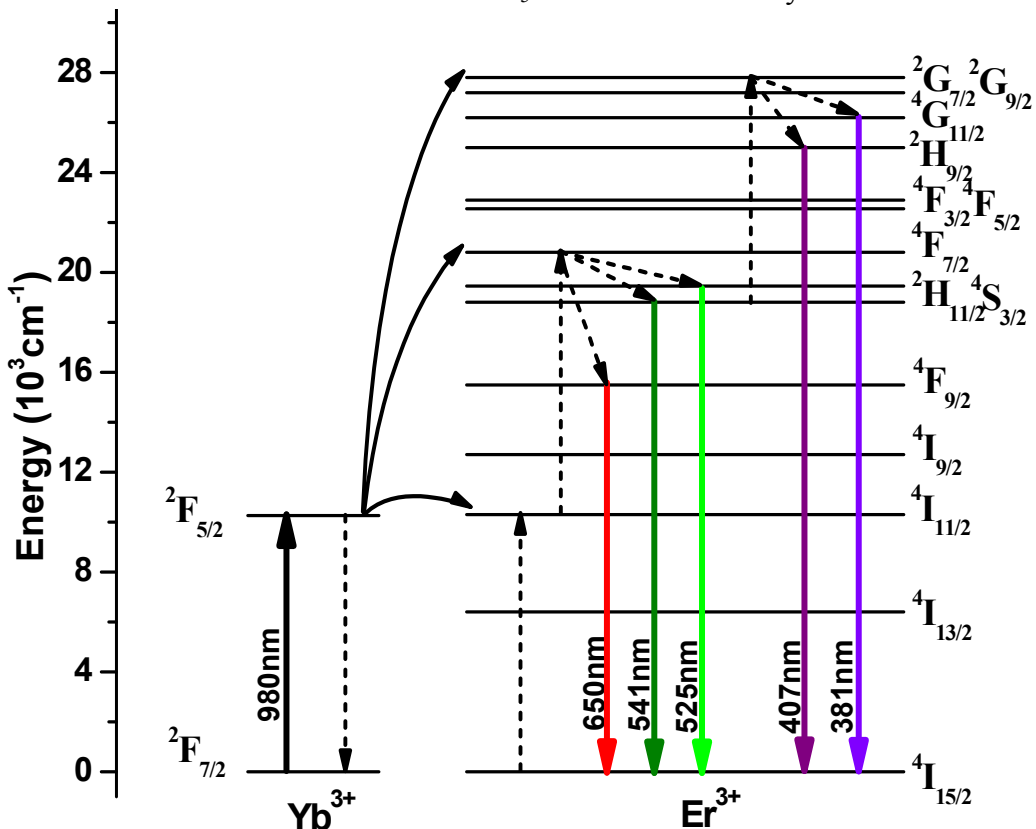


**Figure S9.** Schematic energy-level diagrams, upconversion excitation, and visible emission schemes for the  $\text{BaYF}_5$ :  $\text{Yb}^{3+}$ / $\text{Er}^{3+}$  system.

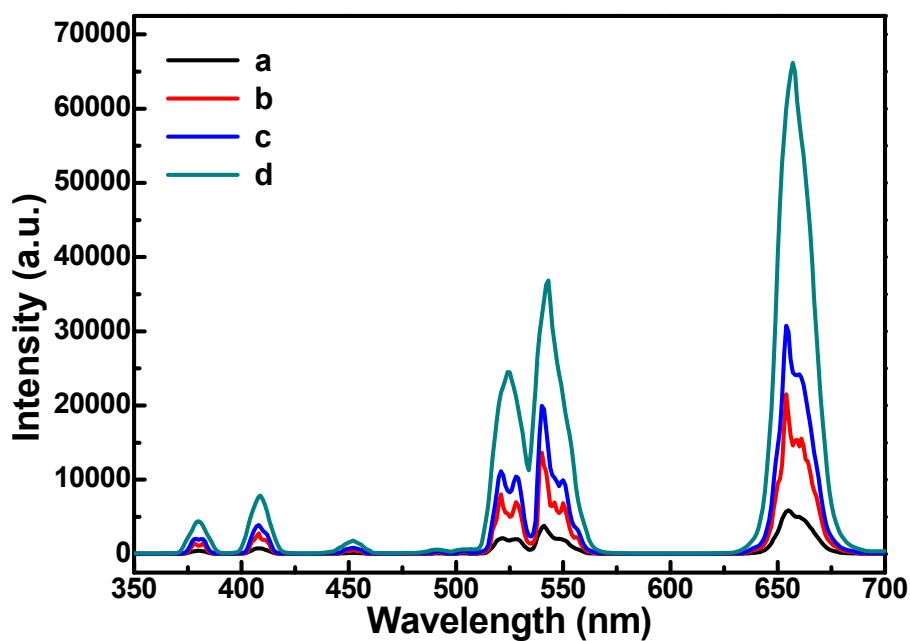


**Figure S10.** Upconversion emission spectra in the wavelength range of 350-700 nm of  $\text{BaYF}_5:18\%\text{Yb}^{3+}/2\%\text{Er}^{3+}$  powders with size of (a) 10-20 nm, (b) 50-70 nm, (c) 100 nm, and (d)  $1\mu\text{m}$  microcrystals. The corresponding TEM images of  $\text{BaYF}_5:18\%\text{Yb}^{3+}/2\%\text{Er}^{3+}$  powders with size of (a) 10-20 nm, (b) 50-70 nm, (c) 100 nm, and (d)  $1\mu\text{m}$  was shown in Figure 2.

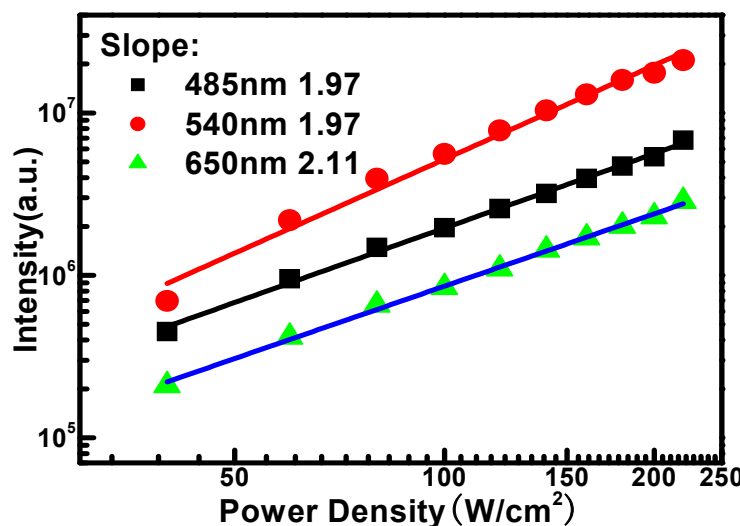


**Figure S11.** The dependence of the intensities of upconversion emissions bands on the power of excitation at 980 nm in the  $\text{BaYF}_5: 18\%\text{Yb}^{3+}/2\%\text{Ho}^{3+}$  system.

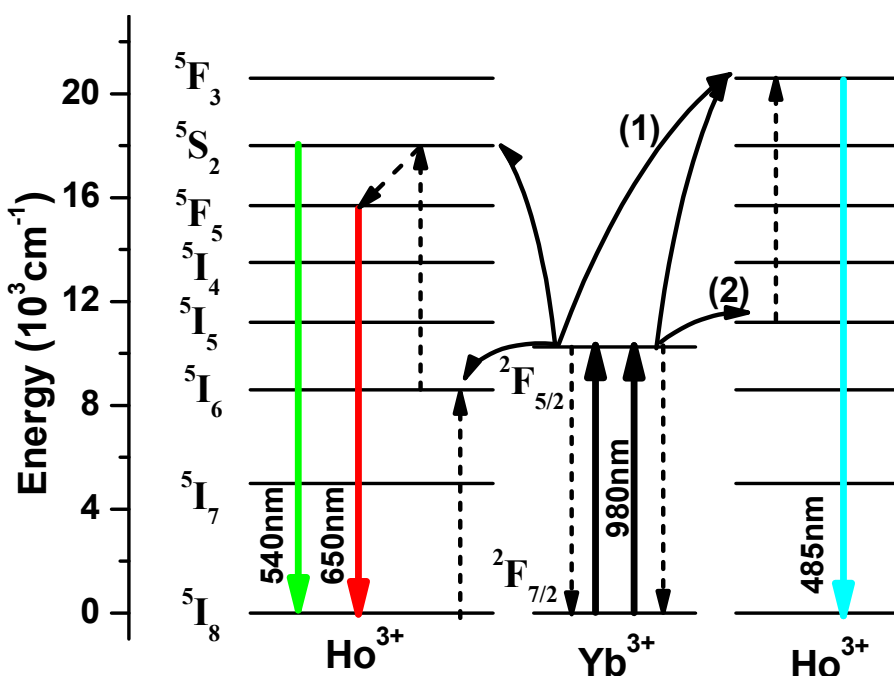


**Figure S12.** Schematic energy-level diagrams, upconversion excitation, and visible emission schemes for the  $\text{BaYF}_5$ :  $\text{Yb}^{3+}$ / $\text{Ho}^{3+}$  system.

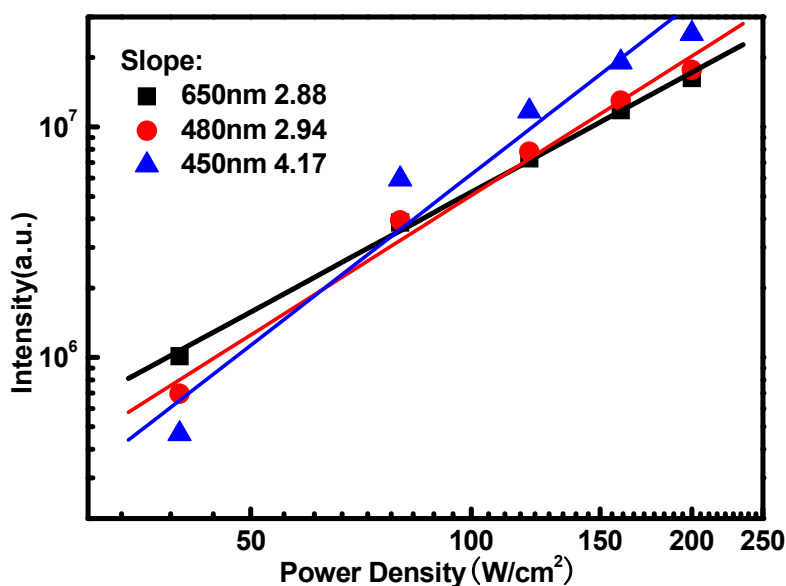


**Figure S13.** The dependence of the intensities of upconversion emissions bands on the power of excitation at 980 nm in the  $\text{BaYF}_5$ : 18% $\text{Yb}^{3+}$ /2% $\text{Tm}^{3+}$  system.

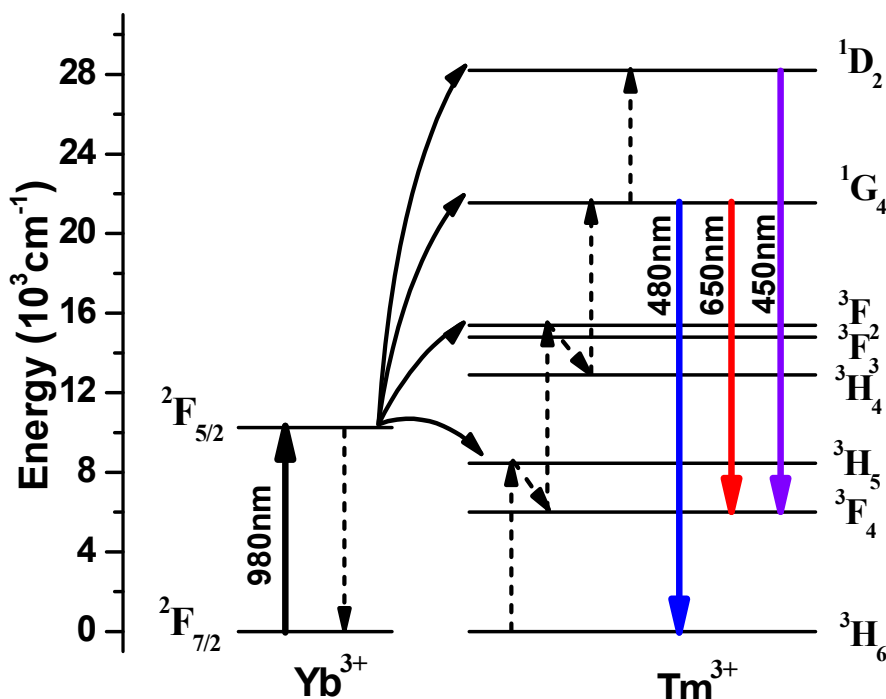


**Figure S14.** Schematic energy-level diagrams, upconversion excitation, and visible emission schemes for the  $\text{BaYF}_5$ :  $\text{Yb}^{3+}/\text{Tm}^{3+}$  system.

**Table S1.** The effect of reaction conditions

Reaction conditions	Size and shape
$\text{RE}^{3+}:\text{EDTA}$	
1:2	10-20nm nanoparticles
1:4	50-70 nm nanoparticles
1:8	100 nm nanoparticles
1:10	1μm cubic microcrystal
pH	
1	5-10nm nanoparticles
3	5-10nm nanoparticles
5	30-40nm nanoparticles
7	250-300nm nanoparticles
$\text{RE}^{3+}:\text{F}^-$	
1:5	10-20nm nanoparticles
1:10	10-20nm nanoparticles
1:15	10-20nm nanoparticles
1:20	10-20nm nanoparticles